THE "SPHERE DUMP" – A NEW LOW-COST HIGH-POWER BEAM DUMP CONCEPT AND A CATALYTIC HYDROGEN-OXYGEN RECOMBINER FOR RADIOACTIVE WATER SYSTEMS*

D. R. Walz and L. R. Lucas
Stanford Linear Accelerator Center, Stanford University, Stanford, California

Summary

This paper reveals a new high-power beam dump concept developed at SLAC. Its principal features are relatively low production costs, simple assembly procedures, compactness, and rather high power absorption capacity. The main power absorption medium is a water-cooled bed of 1 cm diameter aluminum spheres contained in a tube. This "Sphere Beam Dump" is rated at 500 kW and its production costs are compatible with other designs at powers as low as 50 kW. The main features of the dump are discussed with emphasis on heat transfer in the bed of spheres, detection of burnout, and flow and mixing of the coolant. A prototype of such a dump was successfully tested in the electron beam at powers up to 495 kW and at an energy of 18 GeV. The experimental results are discussed and potential applications for other high-power absorbers are indicated.

A catalytic hydrogen-oxygen recombiner for removal of radiolytically produced hydrogen from such a dump and other water-cooled power absorbers is described in the second part of the paper. Such topics as operational parameters, instrumentation, safety, and performance are stressed.

The Sphere Beam Dump

With the achievement of the Stage I design peak current of 50 mA the SLAC linac can now potentially deliver average beam powers up to approximately 600 kW at $E_0 \approx 20$ GeV. The result is an increasing need for beam dumps at intermediate power levels ($600 \geq P_{av} \geq 100$ kW).

High power beam dumps for $P_{av} \leq 2.2$ MW are in operation and were previously described.[1] Unfortunately, application of these dumps is economically feasible only if the experiments are carried out in a permanent beam transport system containing such dumps. These units are bulky and require elaborate radioactive water loops. In the case of temporary beam transport systems, space is usually limited and individual components must be quickly adaptable to various experimental situations. This requires a beam dump that is light and compact, that will be inexpensive, and that can easily accommodate to varying beam configurations. The basic physical requirement for such a dump is adequate shower attenuation in the radial and axial directions. It must allow for certain deviations of the particle beam from its nominal trajectory as might occur from either sudden momentum changes or accidental mis-steering of the beam.

It can be shown that for average incident beam powers significantly in excess of 100 kW, only aluminum or materials with even lower Z are suitable at the shower maximum. Power deposition increases strongly as Z increases and can cause melting or vaporization of the material. However, the length of the dump is minimized by introducing higher Z materials at appropriate distances after the shower maximum.

The Power Absorption Medium

To optimize power absorption and preserve compactness, it is desirable to have a high volume-to-surface area ratio of the power absorption medium.

A sphere is unique in that it has the largest such ratio of any geometry. On the other hand, from a heat transfer point of view, a high surface area-to-volume ratio is most suitable. This ratio varies as 6/D for a sphere, where D is the sphere diameter. Thus, the ratio increases as the sphere becomes smaller. The minimum sphere diameter is determined by the maximum allowable pressure drop through an array or bed of spheres. The pressure drop varies inversely with the sphere diameter. The cooling fluid mass velocity should be high enough to result only in a modest bulk temperature rise and therefore preserve a large subcooling. The latter helps to prevent burnout at relatively low velocities. A bed of spheres is unique in the predictability of the minimum flow volume, and also in the guarantee that the contact of adjacent bodies is a point-contact only. Since there can be no heat transfer to water where surfaces are in contact, the latter have to be minimized.

Another unique feature of the spherical geometry is that the heat flux paths are all essentially radial; and as the heat flux increases as a function of radius from the center to the surface of the sphere (assuming uniformly distributed heat sources), the heat flow area increases also. This keeps temperature gradients, and, therefore, thermal stresses in the material, low. Moreover, a sphere cooled on the outside surface has its highest temperature and stress in the center. The hot center is fully restrained by colder material close to the surface. The sphere can therefore tolerate (without sustaining damage) thermal stresses which are in excess of the material yield or fatigue strength.

The maximum sphere diameter is determined by the maximum heat flux that can be safely transferred by forced convection and nucleate boiling from the sphere surface. Since each sphere is in point-contact with other spheres, the effective heat transfer area is less than the actual sphere surface area. This results in an increase of the effective heat transfer rate off the surface compared to that of a sphere which is uniformly submersed in the cooling fluid.

Important Design Features

A schematic cross section through a sphere dump was published[2] and is shown in Fig. 1. The beam enters the dump through a $\delta = 0.47$ cm thick, dished aluminum head. This window is cooled by the inlet manifold, which discharges part of the water directly onto it. The power deposited for $E_0 = 20$ GeV and $P_{av} = 500$ kW is $P_w = (dE/dx)(P_{av}/E_0)\rho\delta \approx 52$ Watts and no problem exists for any incident beam size.

* Work supported by U. S. Atomic Energy Commission.

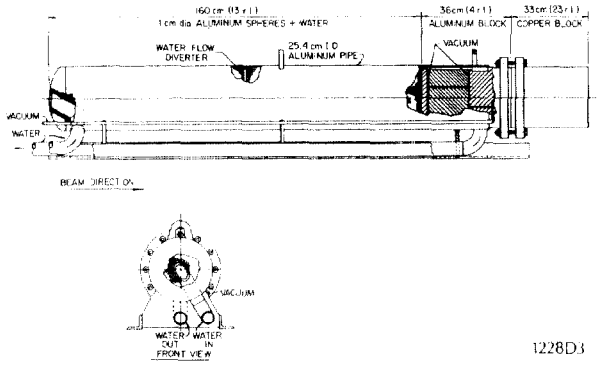

FIG. 1--Schematic of sphere beam dump.

The diameter of the dump was selected to be in accordance with radial shower attenuation in the bed of spheres with an allowance for radial excursions of the beam. High thermal conductivity, low-strength type 1100 aluminum alloy was chosen as the material for the spheres. It exhibits very good corrosion resistance and can be forged easily. The maximum sphere diameter was obtained from heat transfer considerations at the shower maximum. Assuming the same incident beam parameters as for the window, a standard deviation of $0.1 \leq \sigma_b \leq 0.3$ cm, and using existing shower values,[3] it can be shown that the total power deposited in a 1 cm diameter sphere located on the beam centerline and at the shower maximum is $P_s \approx 1.45$ kW. The volume heat source is then $s \approx 2.6$ kW/cm^3 for an assumed uniform power deposition, and the heat flux off the surface and into the water becomes $q'' = 0.45$ kW/cm^2. The effective heat flux is somewhat higher because adjacent spheres are in contact with each other, thus reducing the effective surface area.

Local nucleate boiling heat fluxes of 2 kW/cm^2 were found to be safe for flow parallel to a spot-heated flat plate and for high subcooling.[1] In a bed of spheres this value is expected to be lower due to average rather than local heat fluxes and the particular geometry of the flow passages. The temperature difference from the surface to the center of the sphere can be shown[2] to be $\Delta T \approx 43^{\circ}$C for s = 2.6 kW/cm^3.

The proposed depth of the bed of spheres is 13 radiation lengths (r.ℓ.). This is adequate to partially attenuate the electromagnetic cascade of a 20 GeV, 500 kW beam such that higher Z materials can be employed and water-cooling close to the core of the shower is not an absolute necessity. The maximum density of packing spheres is achieved with the hexagonal close-packed (HCP) structure. The density of packing or packing factor for this case can be shown to be $\epsilon = (\pi\sqrt{2})/6 \approx 0.74$. The actual packing factor calculated from the measured volume of a prototype dump was only 0.583. This is due in particular to imperfect packing at the interface between spheres and the interior surfaces of the container and, to a lesser degree, to imperfect packing throughout the volume (due to friction). It is estimated that $\epsilon \approx 0.65$ in the dump center. One radiation length in this medium of aluminum and water is then equivalent to 12.2 cm.

The bed of spheres is followed by a solid aluminum cylinder. It is peripherally cooled by the water which exits from the bed. The dump is finally terminated with a solid copper cylinder. The copper is used to clean up the remainder of the cascade shower. The amount of power is small enough that the resulting heat can be conducted through the copper cylinder, across a thermal joint into the aluminum cylinder, and through the latter into the water. The thermal joint consists of concentric rings that cause a weak metallic gasket (annealed copper; indium could be used too) to yield due to the clamping force of bolted flanges. The total length of the dump is 40 r.ℓ. (≈230 cm).

A Safety Feature

All existing beam dumps have one shortcoming in common. It is not possible to readily detect a burnout which may have occurred inside the vessel unless it also affects the window or the shell. This could in some instances have serious consequences for personnel and equipment.

In the sphere dump an attempt was made to remedy this situation and provide more safety. The solid aluminum cylinder actually consists of two cylinders with a vacuum cavity in between them. This cavity communicates with a vacuum connection. In case the water flow is off, or too much power is deposited and dissipated in the dump and this leads to destruction of the bed of spheres by either melting or vaporizing, a low-density, low-Z path can be formed. This would shift the shower maximum downbeam and it would cause excessive power deposition in the aluminum cylinder. The result would be formation of a communication hole between the bed of spheres and the vacuum cavity. If the vacuum cavity were, for example, connected to the beam transport vacuum system (which is interlocked) it would provide an immediate external indication of a burnout condition. At this point the cavity is followed by an additional 25 r.ℓ. of material that offers some short term protection.

Some Flow Considerations

For an HCP structure, the flow cross-sectional area for a unit triangle (whose three corners coincide with the geometrical centers of three spheres) becomes $A_0 = r^2(\sqrt{3} - \pi/2) = 0.04$ cm^2, which is 9.25%. The total open area in a 25 cm diameter tube assuming perfect packing and a perfect fit at the interface with the tube is then $A_{0,tot} = 45$ cm^2. The velocity over a sphere for a flow rate of w = 100 gpm becomes then $V_s \approx 4.5$ ft/sec. The bulk temperature rise for $P_{av} = 500$ kW assuming no losses is $\Delta T_w = 19^{\circ}$C. The pressure loss for w = 100 gpm was measured to be $\Delta p = 16$ psig.

A simple flow visualization test was conducted to gain insight into the mixing and flow patterns in the bed of spheres. The apparatus consisted of a section of lucite tubing filled with spheres and placed into a closed-loop water system. An injection nozzle comparable in size to the expected beam diameter and located at the upstream end of the bed served to introduce air bubbles and a dye. The air bubbles were easily swept through at the design mass velocity and no vapor-locking is expected for nucleate boiling heat transfer. The spread-angle of the dye was a little less than the 60° cone angle expected for an HCP structure and seemed to vary but little with velocity and depth of the bed.

It is interesting to mention that at water velocities well below the design level, whole groups of neighboring spheres started to rotate and move within localized pockets of the bed, although originally the bed was rather carefully packed. Imperfect packing, flow turbulence and drag on the spheres as well as reduced friction are responsible. After some period of time the spheres

had rearranged themselves in a closer packing and voids appeared close to the interface with the vessel. Figure 2 shows the front end of the dump used for the experiment described below. The window is removed and the portior of the dump shown on the left hand side was at the bottom during the experiment. The close packing mentioned above as well as imperfect packing on the top (right hand side) and close to the periphery are evident.

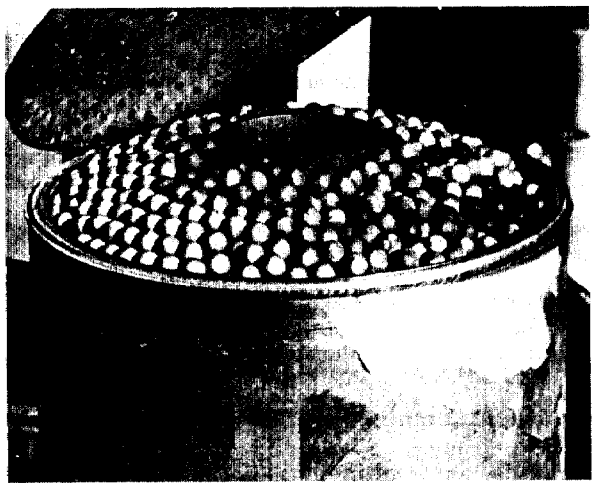

Fig. 2--Front view of sphere beam dump

Power Test of a Prototype Sphere Dump

A prototype of a sphere beam dump was tested in the SLAC beam switchyard on 9-19-68 to gain some understanding of its maximum power absorption capacity and dynamic behavior, and to detect onset of transient conditions which eventually would lead to burnout and destruction of the apparatus. The dump was instrumented with thermocouples to monitor the longitudinal temperature distribution along the nominal beam centerline as a function of beam power delivered by the accelerator. At each measuring location both the temperature of a sphere and the temperature of the cooling water in its vicinity were recorded.

Unfortunately, the Z of the thermocouples (24 gage) was relatively high, particularly compared to that of water and aluminum. Thus, power deposition was significant in the thermocouples and a net heat transfer from them to the water and aluminum occurred. The film temperature drop from the surface of the water thermocouples to the bulk water temperature was substantial for the higher beam powers. The data recorded were therefore higher than the actual local bulk water temperatures that prevailed and should be used only quantitatively.

The dump diameter was only 20 cm since lateral beam excursion could be closely controlled in this experiment. The length was 12.5 r.ℓ. The water flow rate was w = 66 gpm; this resulted in a velocity over the surface of the spheres of V ≈ 4.5 ft/sec. Figure 2 shows the experimental dump after the test.

The nominal electron beam energy was E_0 = 18 GeV. At a pulse repetition rate of 360 pps, the maximum average power delivered by the accelerator and deposited into the dump was P_{av} = 496 kW (this was also a new power record for the accelerator). The shower maximum of the electromagnetic cascade occurs at a depth of[4]

$$T_{max}^{(e^-)} = 1.01\,[\ell n\,(E_0/\epsilon_0) - 1] \quad .$$

For E_0 = 18 GeV and a material critical energy[3] of ϵ_0 = 40 MeV for aluminum, T_{max} = 5.16 r.ℓ. For water, ϵ_0 = 72.8 MeV and T_{max} = 4.55 r.ℓ. With ϵ = 0.65 the shower maximum in the bed of spheres becomes $T_{max} \approx 5.1$ r.ℓ. This is also the area of peak power deposition and thus the area where highest temperatures prevail.

Figure 3 shows the longitudinal temperature distribution of the spheres in the dump for several incident beam powers. As expected, the shape of the curves is similar to shower curves. The major deviation occurs in the attenuation region of the shower, where shower curves exponentially approach zero and the test curves flatten out and asymptotically approach the bulk water temperature after complete mixing has taken place. The highest temperature recorded for each power level occurred at a depth of about 4 r.ℓ. This is in disagreement to the 5.1 r.ℓ. as predicted above. The difference is probably due to a combination of two factors, namely errors in the radial position of the thermocouples located at a depth of 5 and 6 r.ℓ., and a higher than assumed packing factor in the center of the dump.

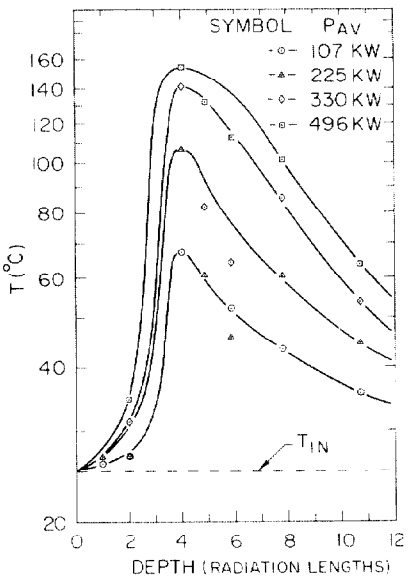

Fig. 3--Longitudinal temperature distribution in the spheres

The longitudinal temperature distribution in water parallel to the beam centerline at a distance of about 1 cm is presented in Fig. 4. These curves distinguish themselves for the ones in Fig. 3 by their much broader peaks, particularly at the higher temperatures. The broadness of the peaks and their depth are easily explained by the fact that a significant amount of power is deposited in the region of exponential shower attenuation. This shows up as a continual temperature rise to a depth where lateral flow and mixing of the water remove more heat from the core of the shower than is deposited by it.

The broken line marked by T_b gives the boiling temperature of water at the local pressure for comparison.

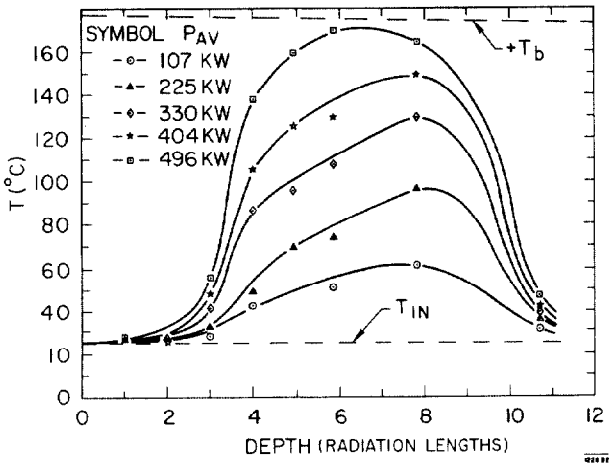

Fig. 4--Longitudinal temperature distribution in the water

It is a function of the pressure drop through the system and thus a function of depth. Heat transfer by nucleate boiling occurred over a wide range of depths for P_{av} = 496 kW as shown by the broad peak approaching T_b. The maximum temperature recorded anywhere in the dump was 170°C. Apart from small (~10°C) fluctuations resulting from the nucleate boiling, temperatures in the dump were stable, and no transients were detected. A detailed analysis of the experiment was published.[5]

Visual inspection of the spheres after the experiment showed no apparent damage. The discoloration visible in Fig. 2 is thought to be a deposit of cupric oxide from the water system.

One beam dump and two high-power protection collimators using beds of spheres are presently in operation at SLAC and a high-power slit is in the design stage. This equipment can safely absorb 500 kW and with a somewhat higher water velocity $P_{av} \approx 600$ kW might be possible.

The Catalytic Hydrogen-Oxygen Recombiner

All high-power absorption devices such as slits, collimators, and beam dumps are water-cooled. In some instances water is used as the primary energy absorbant. The presence of ionizing radiation in water causes radiolysis with subsequent evolution of free hydrogen. Average rates of H_2 evolution of 0.3 liters/(MW sec) were measured and reported.[3,6] The H_2 produced evolves in the gas space on top of the surge tanks of the radioactive water loops and unless removed, the concentrations will build up to the lower explosive limit (LEL ≈ 4% in air at S.T.P.) in rather short order. Dilution and venting is prohibitive due to the amount of radioactivity that would be released into the atmosphere in connection with other (radioactive) gases present. A catalytic hydrogen-oxygen recombiner was developed to solve this problem. The apparatus is directly connected to the closed-loop radioactive water system. It recombines hydrogen and oxygen to form water and all radioactivity is contained in the system.

The Catalyst

The heart of the recombiner is the catalyst. The search for a catalyst was governed by a large number of criteria, the most important being: The catalyst should be efficient in removing H_2; it should not be poisoned by other materials present in the system; operating temperatures should be low to minimize the danger of the catalyst acting as a source of ignition; the catalytic agent should not be lost as a result of operation; the presence of moisture in the gases up to saturation levels should not impair proper functioning; rapid changes of the catalyst surface temperature should not cause either spallation of the catalytic agent from the host material nor shall the latter's integrity be impaired in any way; and finally, it is desirable that the catalyst have a large specific surface area, i.e., a large surface area-to-bed volume ratio.

The catalysts commonly used in commercial applications are of the platinum group of metals. Alumina is frequently used as the catalyst supporting material. This combination was rejected since alumina has a very high modulus of elasticity; sudden temperature changes on the catalyst surface as function of fluctuations in the H_2 concentration can cause spallation of the catalyst coating. A high-nickel stainless steel ribbon compacted into uniformly dense matts was selected. It has been described[7] and is commercially available.* The ribbon dimensions are 0.15 × 0.12 cm and the thickness of the platinum-palladium coating is 3.3×10^{-4} cm. In this application two 15 cm diameter by 3.15 cm thick matts in series and housed in a basket form the catalyst bed.

Description of the Recombiner

An isometric view of a recombiner assembly mounted on top of a surge tank is shown in Fig. 5.

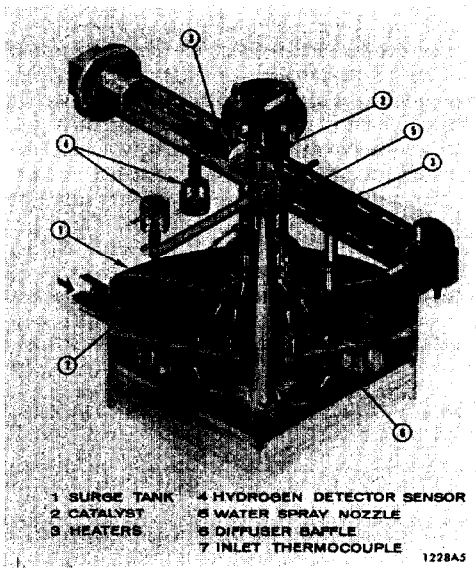

Fig. 5--Artist's concept of the hydrogen recombiner

Water and entrained gases such as H_2 coming from the power absorbers enter tangentially into the surge tank from the left. As the water drips down through the perforated plate the entrained and dissolved gases are partially liberated and collect in the gas space above. The motive power for the gas flow through the recombiner is supplied by a water spray nozzle located inside the

*Universal Oil Products, Air Correction Division, Greenwich, Connecticut.

central tube. It was found that the viscous drag of the high-velocity water droplets in the gas column would induce a head of 2.5 cm of water (static-no-delivery) at low pump speed and 5 cm at high speed. The water for the nozzle is supplied from the discharge side of the pump which serves the main radioactive water loop. Approximately 10 gpm are bypassed. There are no valves and the apparatus is automatically interlocked, i.e., when there is water flow to deliver gases to the surge tank, there is also gas flow in the recombiner.

The gases enter into the annular space formed by two concentric tubes and flow upward. The flow then splits into two horizontal streams and proceeds outward in the lower half of two annuli. Two electrical heaters are housed in the inner tube of these arms. The gas stream must be heated to keep the catalyst temperature above the dew-point. Furthermore, the efficiency of the catalyst increases with increasing temperature; gas inlet temperatures of 65 to 90°C were found to give good results. The heaters are on the air-side of the recombiner, thus, no gaskets are required and the heaters can easily be replaced. The heat is uniformly transmitted to the inside of the cylinder by thermal radiation and a small amount by natural convection. It is then conducted through the wall and by forced convection to the process gas. Note, the horizontal arrangement of the two heater arms is due to vertical space limitations. At the end of the arms the partially heated gases flow into the upper half of the flow annuli, back to the center annulus, and then into the top of the catalyst basket. As the gases flow over the catalyst surface, hydrogen and oxygen are recombined to form water and heat is liberated. Approximately 1 kW of heat is released for each 0.1 liter H_2 recombined per second. The gases then flow past the spray nozzle and down into the surge tank. The nozzle serves not only as an aspirator, but is also a very efficient heat exchanger. The water vapor generated during recombination condenses in the water spray and the cycle is completed.

Instrumentation and Controls

The most important recombiner information is the amount of hydrogen present in the surge tank. High H_2 levels may result from low gas circulation velocity through the catalyst, failure of the catalyst to recombine, lack of oxygen, or low temperature. Because the information is vital, two completely redundant hydrogen sensing systems are used, including two sensing heads, two local relay amplifiers, and two remote amplifiers and readouts in the Data Assembly Building (DAB). Four H_2 detection systems were investigated[8] for potential application in recombiners before a selection was made.* The systems are set to give an audible warning signal at 1% H_2 concentration and an alarm signal at 1.5% H_2. The alarm is interlocked with the electron beam and turns it off.

The H_2 sensing heads are shown at the bottom of the two heater arms. They are located far enough from the central column that the metal temperature is above the dew-point. A cavity is formed by two sintered discs located just above the sensing heads. This cavity is connected to calibration gas bottles by means of a small tube and two check valves. Remote calibration of the sensing heads is thus possible, since the heat exchanger housing and the recombiner are not accessible during operation due to high radiation. A bottle of nitrogen serves to set the zero and a bottle of 1.5% H_2 in air is used to check the alarm.

*Johnson and Williams Model RHSP.

In addition to H_2, the oxygen level in the surge tank is monitored, since proper functioning of the catalyst and the catalytically operating H_2 sensors depends on the presence of O_2. The need for such a system is not yet clearly established. On one hand, during beam start-up only H_2 evolves from the radiolytic decomposition of water and the missing oxygen shows up as a net increase in the H_2O_2 concentration in the water. Only after equilibrium concentration is reached, does H_2O_2 also decompose and H_2 and O_2 evolve at approximately the stoichiometric mixture ratio. During this initial period a net removal of oxygen occurs from the gas space of the surge tank. On the other hand, the latter is vented by a thin tube into the beam transport tunnel to allow for thermal expansion of the water in the system and for filling. Barometric "breathing" and diffusion will tend to keep the O_2 level in the surge tank gas space close to the natural concentration in air (≈21%). The O_2 sensor is a small electrolytic cell, in which O_2 diffuses through a porous membrane into an electrolyte and causes a current to flow between two electrodes proportional to the O_2 concentration. The cell and an amplifier are located outside the radiation area and the gas sample is piped to the cell utilizing the pressure drop across the catalyst bed as driving force. The O_2 level is displayed locally and remotely. If it drops below 15%, a solenoid admits O_2 to the surge tank below the water level. This flow is turned off again after 21% is indicated by the sensor. Should the O_2 level fall below 4%, an audible warning signal is given in the DAB and nitrogen is admitted into the surge tank.

Finally, thermocouples monitor the gas inlet and outlet temperatures at the catalyst bed. It was experimentally established that at least 40°C are needed for successful operation of the catalyst. A low-temperature limit of 65°C was arbitrarily set and if the gas inlet temperature falls below that an audible warning signal is given in the DAB. The normal operating inlet temperature is approximately 70°C. There is also a high-temperature warning at the outlet of the catalyst bed, set at 175°C. The temperatures are displayed both locally and in the DAB, and heater controls are also available at these locations.

Four such recombiner systems are now installed at SLAC, one of which has already successfully operated over a period of two years.

References

1. D.R. Walz, J. Jurow, E. L. Garwin, IEEE Trans. on Nuclear Science, NS-12, No. 3, June 1965.
2. D. Walz, "400-kW sphere beam dump," SLAC-TN-68-7.
3. R. B. Neal, Ed., The Stanford Two-Mile Accelerator, (W. A. Benjamin, Inc., N.Y.); pp. 709-711 (1968).
4. B. Rossi, High-Energy Particles, (Prentice Hall, Inc., N.Y.); p. 257 (1952).
5. D. R. Walz, L. R. Lucas, "Power and flow test of a prototype of the sphere beam dump," SLAC-TN-69-4.
6. D. R. Walz, et al., IEEE Trans. on Nuclear Science, NS-14, No. 3, June 1967.
7. G. M. Brown, et al., "Investigation of catalytic recombination of radiolytic oxygen and hydrogen," General Nuclear Engineering Corp., GNEC-336, April 1964.
8. D. R. Walz, L. R. Lucas, "Hydrogen detection instrumentation for the SLAC hydrogen recombiners," SLAC-TN-67-21.

Acknowledgment

The authors would like to thank Dr. E. J. Seppi for his help in conducting the sphere beam dump experiment.